

On the role of heavy flavor parton distributions at high energy colliders

M. Glück, P. Jimenez-Delgado, E. Reya, C. Schuck

*Universität Dortmund, Institut für Physik
D-44221 Dortmund, Germany*

Abstract

We compare ‘fixed flavor number scheme’ (FFNS) and ‘variable flavor number scheme’ (VFNS) parton model predictions at high energy colliders. Based on our recent LO- and NLO-FFNS dynamical parton distributions, we generate radiatively two sets of VFNS parton distributions where also the heavy quark flavors $h = c, b, t$ are considered as massless partons within the nucleon. By studying the role of these distributions in the production of heavy particles ($h\bar{h}$, $t\bar{t}$, hW^\pm , Higgs-bosons, etc.) at high energy ep , $p\bar{p}$ and pp colliders, we show that the VFNS predictions are compatible with the FFNS ones (to within about 10–20% at LHC, depending on the process) when the invariant mass of the produced system far exceeds the mass of the participating heavy quark flavor.

In a recent publication [1] we updated the dynamical leading order (LO) and next-to-leading order (NLO) parton distributions of [2]. These analyses were undertaken within the framework of the so called ‘fixed flavor number scheme’ (FFNS) where, besides the gluon, only the light quarks $q = u, d, s$ are considered as genuine, i.e. massless partons within the nucleon. This factorization scheme is fully predictive in the heavy quark $h = c, b, t$ sector where the heavy quark flavors are produced entirely perturbatively from the initial light quarks and gluons – as required experimentally, in particular in the threshold region. However, even for very large values of Q^2 , $Q^2 \gg m_{c,b}^2$, these FFNS predictions are in remarkable agreement with DIS data [1, 2] and, moreover, are perturbatively stable, despite the common belief that ‘non-collinear’ logarithms $\ln(Q^2/m_h^2)$ have to be resummed.

In many situations, however, calculations within this factorization scheme become unduly complicated. For example, the single top production process at hadron colliders via W -gluon fusion requires the calculation of the subprocess $ug \rightarrow dt\bar{b}$ at LO and of $ug \rightarrow dt\bar{b}g$ etc. at NLO. It thus becomes expedient to consider for such calculations the so called ‘variable flavor number scheme’ (VFNS) where also the heavy quarks $h = c, b, t$ are taken to be massless partons within the nucleon. In this scheme, the above FFNS calculations simplify considerably, i.e. one needs merely $ub \rightarrow dt$ at LO and $ub \rightarrow dtg$ etc. at the NLO of perturbation theory [3]. The VFNS is characterized by increasing the number n_f of massless partons by one unit at $Q^2 = m_h^2$ starting from $n_f = 3$ at $Q^2 = m_c^2$, i.e. $c(x, m_c^2) = \bar{c}(x, m_c^2) = 0$. The matching conditions at LO and NLO are fixed by continuity relations [4] at the respective thresholds $Q^2 = m_h^2$. Thus the ‘heavy’ $n_f > 3$ quark distributions are perturbatively uniquely generated from the $n_f - 1$ ones via the massless renormalization group Q^2 -evolutions. The running strong coupling can be approximated by the common NLO ‘asymptotic’ solution

$$\frac{\alpha_s(Q^2)}{4\pi} \simeq \frac{1}{\beta_0 \ln(Q^2/\Lambda^2)} - \frac{\beta_1}{\beta_0^3} \frac{\ln \ln(Q^2/\Lambda^2)}{[\ln(Q^2/\Lambda^2)]^2} \quad (1)$$

with $\beta_0 = 11 - 2n_f/3$ and $\beta_1 = 102 - 38n_f/3$, which turns out to be sufficiently accurate [1] for our relevant Q^2 -region, $Q^2 \gtrsim 2 \text{ GeV}^2$. Since $\beta_{0,1}$ are not continuous for different flavor

numbers n_f , the continuity of $\alpha_s(Q^2)$ requires to choose different values for the integration constant Λ for different n_f , $\Lambda^{(n_f)}$, which are fixed by the common $\alpha_s(Q^2)$ matchings at the flavor thresholds $Q = m_{c,b,t}$. Choosing $m_c = 1.3$ GeV, $m_b = 4.2$ GeV and $m_t = 175$ GeV, one obtains $\Lambda_{\overline{\text{MS}}}^{(4,5,6)} = 269.7, 184.5, 72.9$ MeV according to our dynamical NLO($\overline{\text{MS}}$) fit [1] which resulted in $\alpha_s(M_Z^2) = 0.1145$. In LO, where $\beta_1 \equiv 0$, we obtained [1] $\Lambda_{LO}^{(4,5,6)} = 181.8, 138.3, 70.1$ MeV corresponding to $\alpha_s(M_Z^2) = 0.1263$.

Our choice for the input of the ‘heavy’ VFNS distributions are the LO and NLO dynamical FFNS distributions [1] at $Q^2 = m_c^2$. The VFNS predictions at scales $Q^2 \gg m_h^2$ should become insensitive to this, somewhat arbitrary, input selection [5] whose virtues are the fulfillment of the standard sum-rule constraints together with reasonable shapes and sizes of the various input distributions. As we shall see, this expectation is based on the fact that at $Q^2 \gg m_h^2$ the VFNS distributions are dominated by their radiative evolution rather than by the specific input at $Q^2 = m_h^2$. In other words, because of the long evolution distance, input differences get ‘evolved away’ at $Q^2 \gg m_h^2$ where the universal perturbative QCD splittings dominate.

As a first test of the VFNS ‘heavy’ quark distributions we consider charm and bottom electroproduction processes, since deep inelastic structure functions play an instrumental role in determining parton distributions. In Figs. 1 and 2 we compare the VFNS with the FFNS predictions for $F_2^c(x, Q^2)$ and $F_2^b(x, Q^2)$, respectively, using¹ $\mu^2 = Q^2 + 4m_{c,b}^2$ for the FFNS although our results are not very sensitive to this specific choice of the factorization and renormalization scales. As usual, $\mu^2 = Q^2$ in the VFNS. Notice furthermore that the NLO–VFNS predictions for xh (short-dashed curves) are very similar to the ones for $(2e_h^2)^{-1}F_2^h$ (dashed curves) despite the fact that $(2e_h^2)^{-1}F_2^h = (1 + \alpha_s C_q) \otimes h + \frac{1}{2} \alpha_s C_g \otimes g$, i.e. the $\mathcal{O}(\alpha_s)$ quark and gluon contributions almost cancel. As expected [6] the discrepancies

¹Notice that here and in the following $\mu_R = \mu_F \equiv \mu$ where μ_R and μ_F are the renormalization and factorization scales, respectively. This choice is dictated by the fact that our (and all other presently available) parton distributions were determined and evolved with $\mu_R = \mu_F$, i.e. with the commonly adopted standard evolution equations.

between the predictions for $xh(x, Q^2)$ in the VFNS and for $(2e_h^2)^{-1}F_2^h(x, Q^2)$ in the FFNS in the relevant kinematic region (small x , large Q^2) never disappear and can amount to as much as about 30% at very small- x , even at $W^2 \equiv Q^2(\frac{1}{x} - 1)$ far above threshold, i.e. $W^2 \gg W_{th}^2 = (2m_h)^2$. This is due to the fact that here the ratio of the threshold energy $W_{th} \equiv \sqrt{\hat{s}_{th}}$ of the massive subprocess ($\gamma^*g \rightarrow h\bar{h}$, etc.) and the mass of the produced heavy quark $\sqrt{\hat{s}_{th}}/m_h = 2$ is not sufficiently high to exclude significant contributions from the threshold region. Even for the lightest heavy quark, $h = c$, such non-relativistic ($\beta_c = |\vec{p}_c|/E_c \lesssim 0.9$) threshold region contributions to $F_2^h(x, Q^2)$ are sizeable for $W^2 \lesssim 10^6$ GeV² due to significant $\beta_c < 0.9$ contributions, and the situation becomes worse for $h = b$ (cf. Fig. 4 of [6]). This is in contrast to processes where one of the produced particles is much heavier than the other one, like the weak CC contribution [7, 8] $W^+g \rightarrow t\bar{b}$ to F_2^{CC} . Here $\sqrt{\hat{s}_{th}}/m_b = (m_t + m_b)/m_b \gg 1$ and the extension of the threshold region where $\beta_b \lesssim 0.9$, being proportional to $m_b/\sqrt{\hat{s}_{th}} \ll 1$, is strongly reduced as compared to $m_h/(2m_h) = 0.5$ in the former case of $h\bar{h}$ production. Thus the single top production rate in $W^+g \rightarrow t\bar{b}$ is dominated by the (beyond-threshold) relativistic region where $\beta_b > 0.9$ and therefore is expected to be well approximated by $W^+b \rightarrow t$ where b is an effective massless parton within the nucleon. In Fig. 3 we compare the LO FFNS [7, 8] predictions for $\frac{1}{2}F_{2,t\bar{b}}^{CC}(x, Q^2)$ with the corresponding VFNS ones for $\xi b(\xi, Q^2 + m_t^2)$ where the latter refers to the $W^+b \rightarrow t$ transition using the slow rescaling variable [9] $\xi = x(1 + m_t^2/Q^2)$ with $m_t = 175$ GeV. For $F_{2,t\bar{b}}^{CC}(x, Q^2)$ we used $\mu_R^2 = \mu_F^2 \equiv \mu^2 = Q^2 + (m_t + m_b)^2$. (Notice that the fully massive NLO FFNS QCD corrections to $W^+g \rightarrow t\bar{b}$ are unfortunately not available in the literature.) As expected the differences between the two schemes are here less pronounced than in the case of $c\bar{c}$ and $b\bar{b}$ electroproduction in Figs. 1 and 2. These results indicate that one may resort to the simpler VFNS with its massless $h(x, \mu^2)$ distributions to estimate rather reliably the production rates of heavy quarks, gauge bosons, Higgs scalars, etc. at Tevatron and LHC energies.

As a next test of these VFNS distributions we therefore turn to hadronic W^\pm production

and present in Fig. 4 their NLO predictions for $\sigma(p\bar{p} \rightarrow W^\pm X)$ as compared to the data [10, 11, 12, 13, 14] and to predictions based on the NLO CTEQ6.5 distributions [15]. Also shown in this figure is a comparison of our LO FFNS and VFNS predictions. Although quantitatively slightly different, the dominant light quark contributions in the FFNS ($u\bar{d} \rightarrow W^+$, $u\bar{s} \rightarrow W^+$, etc.) are due to the same subprocesses as in the VFNS, but the relevant heavy quark contributions have been calculated via $g\bar{s}(\bar{d}) \rightarrow \bar{c}W^+$, $gu \rightarrow bW^+$, etc. as compared to $c\bar{s}(\bar{d}) \rightarrow W^+$, $\bar{b}u \rightarrow W^+$ etc. in the VFNS. Here we again expect the VFNS with its effective massless ‘heavy’ quark distributions $h(x, \mu^2)$ to be adequate, since non-relativistic contributions from the threshold region in the FFNS are suppressed due to $\sqrt{\hat{s}_{th}}/m_{c,b} \simeq M_W/m_{c,b} \gg 1$. The LO gluon induced heavy quark contributions to W^\pm production in the FFNS are obtained from a straightforward calculation of the differential cross section [16] $d\hat{\sigma}(\hat{s})/d\hat{t}$ which yields

$$\begin{aligned} \hat{\sigma}(\hat{s})^{gs \rightarrow cW^-} = \frac{G_F}{\sqrt{2}} \frac{\alpha_s(\mu^2)}{6} |V_{cs}|^2 \frac{M_W^2}{\hat{s}} \left\{ \left(1 + \frac{m_c^2}{2M_W^2}\right) \left[\frac{\sqrt{\lambda}}{2}(1 + 7\Delta)\right] \right. \\ \left. + (1 - 2\Delta + 2\Delta^2) \ln \frac{1 - \Delta + \sqrt{\lambda}}{1 - \Delta - \sqrt{\lambda}} \right\} - \frac{m_c^2}{M_W^2} \sqrt{\lambda} \end{aligned} \quad (2)$$

where

$$\Delta = \frac{M_W^2 - m_c^2}{\hat{s}} \quad , \quad \lambda = \left[1 - \frac{(m_c + M_W)^2}{\hat{s}}\right] \left[1 - \frac{(m_c - M_W)^2}{\hat{s}}\right] ,$$

$\alpha_s(\mu^2) = 4\pi/[9 \ln(\mu^2/\Lambda_{LO}^{(3)})]$ and the relevant CKM matrix element(s) $V_{qq'}$ are taken from [17]. The corresponding total W^\pm hadronic production cross section relevant for Fig. 4 is then given by

$$\sigma^{p\bar{p} \rightarrow cW^\pm X}(s) = \int_\tau^1 dx_1 \int_{\tau/x_1}^1 dx_2 [g(x_1, \mu^2)s(x_2, \mu^2) + (1 \leftrightarrow 2)] \hat{\sigma}(x_1 x_2 s) \quad (3)$$

where $s(x, \mu^2) = \bar{s}(x, \mu^2)$ with $\mu^2 = \mathcal{O}(M_W^2)$ and $\tau = (m_c + M_W)^2/s$. Unfortunately, the NLO($\overline{\text{MS}}$) corrections to this (massive quark) FFNS cross section are again not available in the literature. Only quantitative LO and NLO results for the analogous process $gb \rightarrow tW^-$ have been presented in [18], but questioned in [19]. Here we just mention that we fully confirm the LO results for Wt production obtained in [19] at Tevatron and LHC energies.

Taking into account that the $K \equiv \text{NLO}/\text{LO}$ factor is expected [19] to be in the range of $1.2 - 1.3$, our LO–FFNS predictions in Fig. 4 imply equally agreeable NLO predictions as the (massless quark) NLO–VFNS ones [20] shown by the solid and dashed–dotted curves in Fig. 4.

In Table 1 we present our VFNS and FFNS predictions for W^\pm production at LHC and compare the relevant subprocess contributions to $\sigma(pp \rightarrow W^\pm X)$ at $\sqrt{s} = 14$ TeV. The light quark fusion contributions in the ud and us sector turn out to be somewhat larger in the FFNS than in the VFNS which is due to the fact that the u, d, s (and the gluon) distributions are evolved for fixed $n_f = 3$ in the FFNS. More interesting, however, are the subprocesses involving heavy quarks. Here the LO–VFNS predictions are compatible, to within less than 15%, with the LO–FFNS predictions based on the gluon induced fixed order in α_s subprocesses $gu \rightarrow bW$, $gd \rightarrow cW$ and in particular on the sizeable CKM non-suppressed $gs \rightarrow cW$ contribution. As mentioned above, the NLO corrections to these latter heavy quark contributions cannot be calculated for the time being. However, since these contributions amount to about only 15% of the total FFNS results for W^\pm production (being dominated by the light ud and us fusions in Table 1), we can *safely* employ the expected [19] K factor of $K \simeq 1.2$ for the relevant $gd \rightarrow cW$ and $gs \rightarrow cW$ LO contributions in Table 1 for obtaining the total NLO–FFNS predictions without committing any significant error. The resulting total rate for $W^+ + W^-$ production at LHC of 192.7 ± 4.7 nb is comparable to our NLO–VFNS prediction in Table 1 of 186.5 ± 4.9 nb where we have added the $\pm 1\sigma$ uncertainties implied by our dynamical parton distributions [1].² This latter prediction reduces to 181.0 nb when using the smaller scale $\mu^2 = M_W^2/4$. The scale uncertainties of our predictions are defined by taking $M_W/2 \leq \mu \leq 2M_W$, using $M_W = 80.4$ GeV, which gives rise to the upper limits ($\mu = 2M_W$) and lower limits ($\mu = M_W/2$) of our predicted cross sections. In this way we obtain the following total

²Using ‘standard’ FFNS parton distributions [1] instead of the dynamical ones for generating the VFNS distributions, the dynamical NLO–VFNS prediction of 186.5 nb slightly increases to 190.7 nb.

uncertainty estimates of our NLO predictions at LHC:

$$\sigma(pp \rightarrow W^+ + W^- + X) = \begin{cases} 186.5 \pm 4.9_{\text{pdf}} \begin{smallmatrix} +4.8 \\ -5.5 \end{smallmatrix} |_{\text{scale}} & \text{nb , VFNS} \\ 192.7 \pm 4.7_{\text{pdf}} \begin{smallmatrix} +3.8 \\ -4.8 \end{smallmatrix} |_{\text{scale}} & \text{nb , FFNS} \end{cases} \quad (4)$$

and, for completeness, at LO

$$\sigma(pp \rightarrow W^+ + W^- + X) = \begin{cases} 162.1 \pm 3.9_{\text{pdf}} \begin{smallmatrix} +20.3 \\ -21.8 \end{smallmatrix} |_{\text{scale}} & \text{nb , VFNS} \\ 166.7 \pm 4.0_{\text{pdf}} \begin{smallmatrix} +17.3 \\ -19.0 \end{smallmatrix} |_{\text{scale}} & \text{nb , FFNS} \end{cases} \quad (5)$$

where the subscript pdf refers to the 1σ uncertainties of our parton distribution functions [1]. For comparison, the NLO–VFNS prediction of CTEQ6.5 [15] is 202 nb with an uncertainty of 8%, taking into account a pdf uncertainty of slightly more than 2σ . Similarly, MRST [21] predict about 194 nb. From these results we conclude that, for the time being, the total W^\pm production rate at LHC can be safely predicted within an uncertainty of about 10% irrespective of the factorization scheme.

It is also interesting to study the dependence of the FFNS predictions for the contributions to W^\pm production involving heavy quarks on the chosen scale μ as shown in Figs. 5 and 6. In these figures we compare the $gs \rightarrow cW$ initiated production rates in the FFNS with the quark fusion $cs \rightarrow W$ ones in the VFNS and similarly the $gd \rightarrow cW$ ones with the $cd \rightarrow W$ fusion, respectively. These factorization scheme dependencies are rather mild for the LO–FFNS predictions, in contrast to the situation for the LO–VFNS predictions which stabilize, as expected, at NLO. The mild μ dependence is similar to the situation encountered in tW production [19] via the subprocess $gb \rightarrow tW^-$.

A similar situation where the invariant mass of the produced system sizeably exceeds the mass of the participating heavy quarks is encountered in (heavy) Higgs H production accompanied by two heavy b -quarks, for example. Here $H = H_{\text{SM}}^0$; h^0 , H^0 , A^0 denotes the SM Higgs-boson or a light scalar h^0 , a heavy scalar H^0 and a pseudoscalar A^0 of supersymmetric theories with $M_H \gtrsim 100$ GeV. In the FFNS the dominant production mechanism starts with the LO subprocess $gg \rightarrow b\bar{b}H$ ($q\bar{q} \rightarrow b\bar{b}H$ is marginal), to be

compared with the $b\bar{b}$ fusion subprocess in the VFNS starting with $b\bar{b} \rightarrow H$ at LO. Again, $\sqrt{\hat{s}_{th}}/m_b = (2m_b + M_H)/m_b \simeq M_H/m_b \gg 1$ in the FFNS which indicates that the simpler LO and NLO(NNLO) VFNS $b\bar{b}$ fusion subprocesses do provide reliable predictions. Within the scale uncertainties it turns out that the FFNS and VFNS predictions at NLO are compatible [22, 23, 24, 25], using the MRST2002 and CTEQ6 parametrizations of the relevant parton distributions [21, 26]. This result holds for scale choices $\mu_{R,F} = (\frac{1}{8} \text{ to } \frac{1}{2})\sqrt{\hat{s}_{th}}$ with $\sqrt{\hat{s}_{th}}/4$ being considered as a suitable ‘central’ choice in $b(x, \mu_F^2)$ for calculations based on the $b\bar{b}$ fusion process in the VFNS.³ It should, however, be mentioned that the VFNS rates somewhat exceed [22, 23, 24, 25] the corresponding FFNS Higgs–boson production rates by about³ 10–20%.

Finally let us note that all our results and comparisons concerning the VFNS hold irrespective of the specific parametrizations used for the ‘heavy’ $h(x, \mu^2)$ distributions: when comparing our VFNS distributions, generated from using our dynamical distributions [1] as input, with the ones of CTEQ6 [26] or CTEQ6.5 [15] the relevant ratios $c(x, M_W^2)_{\text{CTEQ}}/c(x, M_W^2)_{\text{GJR-VFNS}}$ and $b(x, m_t^2)_{\text{CTEQ}}/b(x, m_t^2)_{\text{GJR-VFNS}}$ vary, for $10^{-4} \lesssim x \lesssim 0.1$, at most between 0.9 – 1.1 at LO and NLO. Similar results hold when using other VFNS distributions, e.g., those of [5]. This is illustrated more quantitatively in Fig. 7 where we compare our c - and b -distributions, together with the important gluon-distribution, with the ones of CTEQ6 [26] and CTEQ6.5 [15] in the sea- and gluon-relevant x -region $x \lesssim 0.3$ at $Q^2 = M_W^2$. The ratios for the light u - and d -distributions are even closer to 1 than the ones shown in Fig. 7, typically between 0.95 and 1.05 which holds in particular for the CTEQ6 distributions when compared to our ones. Incidentally the VFNS under consideration and commonly used [5, 26] is also referred to as the zero-mass VFNS. Sometimes one uses an improvement on this, now known as the general-mass VFNS [15, 21, 27, 28, 29, 30], where mass-dependent corrections are maintained in the hard cross sections. This latter factorization scheme interpolates between the strict zero-mass VFNS,

³The *independent* variation of μ_F and μ_R considered in [22, 23, 24, 25] is, as mentioned before, not strictly compatible with the utilized parton distributions determined and evolved according to $\mu_R = \mu_F$.

used in our evolution to $Q^2 \gg m_h^2$, and the (experimentally required) FFNS used for our input at $Q^2 = m_h^2$. As expected and shown in Fig. 7, scheme (input) differences at lower $Q^2 = \mathcal{O}(m_h^2)$ only marginally affect the asymptotic results at $Q^2 = M_W^2 \gg m_{c,b}^2$ where the CTEQ6.5 parametrizations [15] (corresponding to a general-mass VFNS) become very similar to the ones of CTEQ6 [26] and our GJR-VFNS (corresponding to the zero-mass VFNS). As stated repeatedly before, this is essentially due to the dominance of the large evolution effects over the minor differences involved at the lower scales, e.g. at $Q^2 = \mathcal{O}(m_h^2)$. These asymptotic similarities are particularly relevant for the simplified (vanishing $m_{c,b}$) calculations of the production rates of very massive particles where massive c - and b -quark threshold region contributions are strongly suppressed.

To summarize, we generated radiatively two sets of VFNS parton distributions, based on our recent LO and NLO dynamical parton distributions [1] obtained in the FFNS. Within the VFNS additional heavy quark distributions $h(x, Q^2) = \bar{h}(x, Q^2)$ are generated perturbatively via the common massless Q^2 -evolution equations by imposing the boundary conditions $h(x, Q^2 = m_h^2) = 0$ for $h = c, b, t$. We have confronted the VFNS and FFNS predictions in situations where the invariant mass of the produced system ($h\bar{h}$, $t\bar{t}$, cW , tW , Higgs-bosons, etc.) does not exceed or exceeds by far the mass of the participating heavy flavor. In the former case (e.g. F_2^c in deep inelastic $c\bar{c}$ production where $\sqrt{\hat{s}_{th}}/m_c = 2$) the VFNS predictions deviate from the FFNS ones by up to about 30% even at $Q^2 \gg m_c^2$. In the latter case (e.g. $F_{2,t\bar{b}}^{CC}$ in deep inelastic weak charged current $t\bar{b}$ production where $\sqrt{\hat{s}_{th}}/m_b \simeq m_t/m_b \gg 1$) these deviations are appreciably less, within about 10%, which is within the margins of renormalization and factorization scale uncertainties. As a further example of the agreement between the VFNS and FFNS predictions in situations where the invariant mass of the produced system far exceeds $m_{c,b}$ we considered the corresponding W^\pm boson production rates at the Tevatron and at the large hadron collider (where e.g. $\sqrt{\hat{s}_{th}}/m_{c,b} \simeq M_W/m_{c,b} \gg 1$ for cW and bW production, respectively). For $\sqrt{s} = 14$ TeV the NLO-FFNS predicts $\sigma(pp \rightarrow W^+ + W^- + X) \simeq 192.7$ nb with an uncertainty of 5%, to

be compared with the NLO–VFNS prediction of 186.5 nb and an uncertainty of 6%. The cited uncertainties include also the scale uncertainties due to varying the renormalization and factorization scales $\mu_R = \mu_F$ between $M_W/2$ and $2M_W$. (It should be emphasized again that the scale choice $\mu_R = \mu_F$ is dictated by all presently available parton distributions which have been determined and evolved according to $\mu_R = \mu_F$.) Furthermore, a similar agreement is obtained for hadronic (heavy) Higgs–boson production when the dominant FFNS subprocess $gg \rightarrow b\bar{b}H$ (where $\sqrt{\hat{s}_{th}}/m_b = (2m_b + M_H)/m_b \gg 1$) is compared with the VFNS b –quark fusion subprocess ($b\bar{b} \rightarrow H$, etc.).

These results indicate that the simpler VFNS with its effective treatment of heavy quarks (c, b, t) as massless partons can be employed for calculating processes where the invariant mass of the produced system is sizeably larger than the mass of the participating heavy quark flavor. The uncertainty of such calculations is process (and somewhat energy) dependent when compared with the predictions of the FFNS where the effects of finite heavy quark masses are nowhere neglected. Taking into account the uncertainties of parton distributions and scale choices as well, the total W^\pm production rate at LHC can be predicted within an uncertainty of about 10%, which becomes significantly smaller at the Tevatron. Similarly the Higgs production rates at LHC are predicted with an uncertainty of 10–20% where the VFNS production rates exceed the FFNS ones by about 20% at LHC.

A FORTRAN code (grid) containing our new LO and NLO($\overline{\text{MS}}$) light ($u, d, s; g$) and heavy (c, b, t) parton distributions in the VFNS, generated from our recent dynamical ones in the FFNS [1], can be obtained on request or directly from <http://doom.physik.uni-dortmund.de> .

Acknowledgements

We thank J. Campbell for a clarifying correspondence. This work has been supported in part by the ‘Bundesministerium für Bildung und Forschung’, Berlin/Bonn.

References

- [1] M. Glück, P. Jimenez–Delgado, E. Reya, *Eur. Phys. J.* **C53** (2008) 355
- [2] M. Glück, E. Reya, A. Vogt, *Eur. Phys. J.* **C5** (1998) 461
- [3] T. Stelzer, Z. Sullivan, S. Willenbrock, *Phys. Rev.* **D56** (1997) 5919
- [4] J.C. Collins, W.K. Tung, *Nucl. Phys.* **B278** (1986) 934
- [5] S.I. Alekhin, *Phys. Rev.* **D68** (2003) 014002
- [6] M. Glück, E. Reya, M. Stratmann, *Nucl. Phys.* **B422** (1994) 37
- [7] M. Glück, R.M. Godbole, E. Reya, *Z. Phys.* **C38** (1988), 441; **C39** (1988) 590(E)
- [8] U. Baur, J.J. van der Bij, *Nucl. Phys.* **B304** (1988) 451
- [9] R.M. Barnett, *Phys. Rev. Lett.* **36** (1976) 1163;
R. Barbieri, J. Ellis, M.K. Gaillard, G.G. Ross, *Nucl. Phys.* **B117** (1976) 50
- [10] C. Albajar et al., UA1 Collaboration, *Z. Phys.* **C44** (1989) 15
- [11] J. Alitti et al., UA2 Collaboration, *Phys. Lett.* **B276** (1992) 365
- [12] B. Abbott et al., DØ Collaboration *Phys. Rev.* **D61** (2000) 072001
- [13] F. Abe et al., CDF Collaboration, *Phys. Rev. Lett.* **69** (1992) 28
- [14] A. Abulencia et al., CDF Collaboration, *J. Phys.* **G34** (2007) 2457
- [15] W.K. Tung et al., CTEQ Collaboration, *JHEP* 02(2007)053
- [16] F. Halzen, C.S. Kim, *Int. J. Mod. Phys.* **A2** (1987) 1069
- [17] W.-M. Yao et al., Particle Data Group, *J. Phys.* **G33** (2006) 1
- [18] S. Zhu, *Phys. Lett.* **B524** (2002) 283; **B537** (2002) 351(E)

- [19] J. Campbell, F. Tramontano, *Nucl. Phys.* **B726** (2005) 109
- [20] R. Hamberg, W.L. van Neerven, T. Matsuura, *Nucl. Phys.* **B359** (1991) 343
- [21] A.D. Martin et al., *Eur. Phys. J.* **C23** (2002) 73; *Phys. Lett.* **B531** (2002) 216
- [22] S. Dittmaier, M. Krämer, M. Spira, *Phys. Rev.* **D70** (2004) 074010
- [23] S. Dawson, C.B. Jackson, L. Reina, D. Wackerroth, *Phys. Rev. Lett.* **94** (2005) 031802
- [24] J. Campbell et al., ‘Physics at TeV Colliders’ (3rd Les Houches Workshop, 2003),
hep-ph/0405302
- [25] S. Dawson, C.B. Jackson, L. Reina, D. Wackerroth, *Mod. Phys. Lett.* **A21** (2006) 89
- [26] J. Pumplin et al., CTEQ Collaboration, *JHEP* **07** (2002) 012
- [27] S. Kretzer et al., *Phys. Rev.* **D69** (2004) 114005
- [28] M.A.G. Aivazis et al., *Phys. Rev.* **D50** (1994) 3102
- [29] M. Buza et al., *Eur. Phys. J.* **C1** (1998) 301;
A. Chuvakin, J. Smith, and W.L. van Neerven, *Phys. Rev.* **D61** (2000) 096004
- [30] R.S. Thorne and R.G. Roberts, *Phys. Rev.* **D57** (1998) 6871;
R.S. Thorne, *Phys. Rev.* **D73** (2006) 054019

$\sigma^{pp \rightarrow WX} \text{ (nb)}, \sqrt{s}=14 \text{ TeV}$						
	VFNS: NLO (LO)			FFNS: NLO (LO)		
	W^+	W^-	$W^+ + W^-$	W^+	W^-	$W^+ + W^-$
ud	87.7 (77.6)	60.6 (52.6)	148.3 (130.3)	93.3 (81.9)	64.6 (55.7)	157.9 (137.6)
us	3.9 (3.3)	1.3 (1.2)	5.3 (4.5)	4.2 (3.5)	1.5 (1.3)	5.7 (4.8)
ub	$7.3 (7.0) \times 10^{-4}$	$2.3 (2.2) \times 10^{-4}$	$9.6 (9.2) \times 10^{-4}$	$- (6.5) \times 10^{-4}$	$- (1.8) \times 10^{-4}$	$- (8.3) \times 10^{-4}$
cd	1.3 (1.1)	2.3 (2.0)	3.6 (3.1)	- (1.0)	- (2.0)	- (3.0)
cs	14.7 (12.2)	14.7 (12.2)	29.4 (24.3)	- (10.6)	- (10.6)	- (21.3)
cb	$1.5 (1.4) \times 10^{-2}$	$1.5 (1.4) \times 10^{-2}$	$2.9 (2.7) \times 10^{-2}$	-	-	-
total	107.5 (94.2)	79.1 (67.9)	186.5 (162.1)	$\simeq 111.4 (97.0)$	$\simeq 81.2 (69.6)$	$\simeq 192.7 (166.7)$
						total

Table 1: NLO(LO) VFNS and FFNS predictions for W^\pm production at LHC. The FFNS parton distributions are taken from [1] which form the basis for generating the ones in the VFNS including the ‘heavy’ quark distributions $c(x, \mu^2) = \bar{c}(x, \mu^2)$ and $b(x, \mu^2) = \bar{b}(x, \mu^2)$ taking $\mu = M_W$. The uncertainties implied by different scale choices are summarized in eqs. (4) and (5). The total NLO–FFNS rates have been obtained by adopting an expected [19] K -factor of 1.2 for the subleading gluon initiated LO rates involving the heavy c and b quarks.

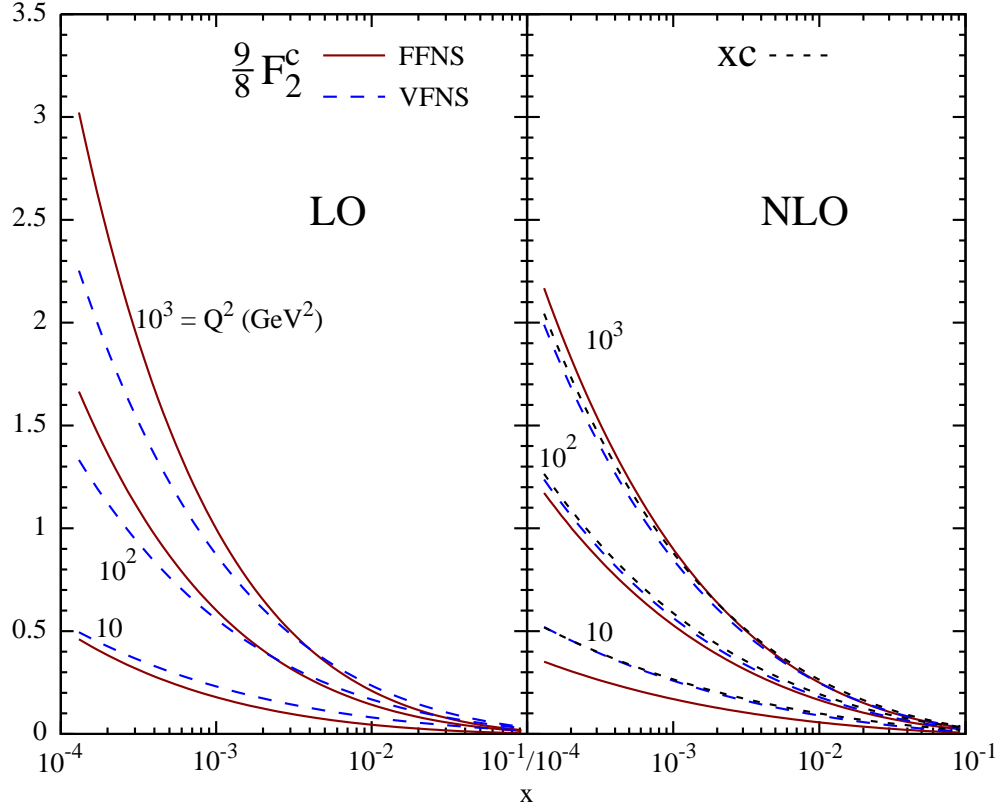


Figure 1: The predicted x -dependencies of $\frac{9}{8}F_2^c(x, Q^2)$ in the FFNS and VFNS at some typical fixed values of Q^2 . For the FFNS the renormalization and factorization scales are chosen to be $\mu_R^2 = \mu_F^2 \equiv \mu^2 = Q^2 + 4m_c^2$ with $m_c = 1.3 \text{ GeV}$, and, as usual, $\mu^2 = Q^2$ for the VFNS. The NLO-VFNS charm distribution is given by $xc(x, Q^2)$ as shown by the short-dashed curves.

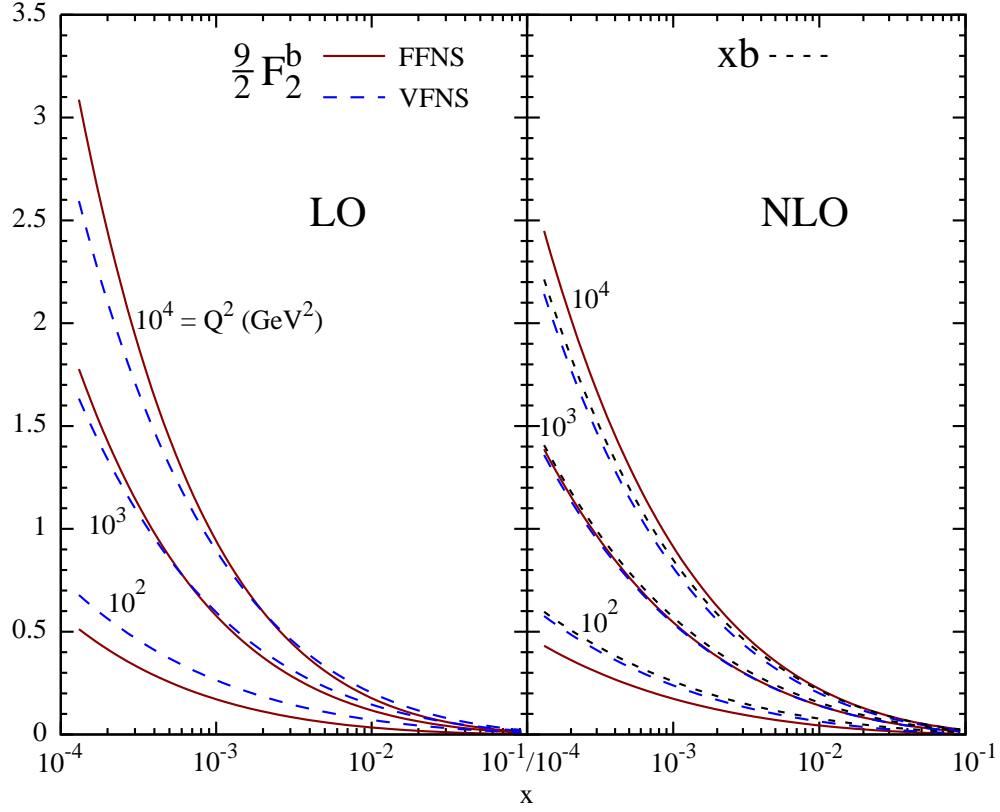


Figure 2: As in Fig. 1 but for bottom production, i.e. $\frac{9}{2} F_2^b(x, Q^2)$, choosing $\mu_R^2 = \mu_F^2 \equiv \mu^2 = Q^2 + 4m_b^2$ with $m_b = 4.2 \text{ GeV}$ for the FFNS. The short-dashed curves show the NLO-VFNS bottom distribution $xb(x, Q^2)$.

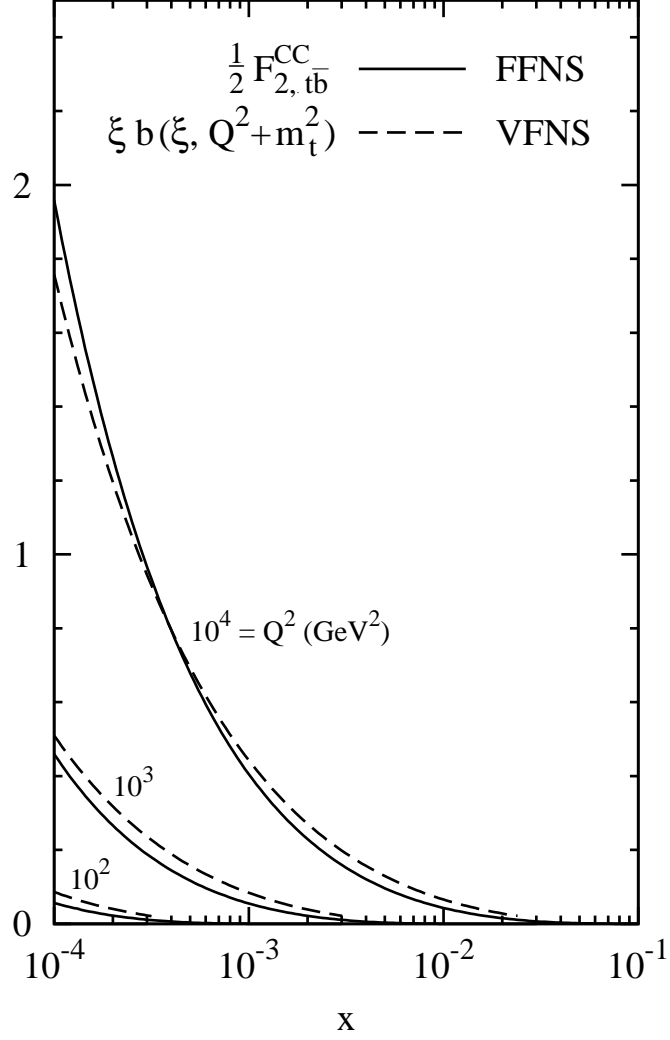


Figure 3: LO predictions for the x -dependencies of the weak charged current structure function $\frac{1}{2} F_{2,t\bar{b}}^{CC}(x, Q^2)$ for $t\bar{b}$ production in the FFNS at some typical fixed values of Q^2 . The momentum scale is chosen to be $\mu_R^2 = \mu_F^2 \equiv \mu^2 = Q^2 + (m_t + m_b)^2$ with $m_t = 175$ GeV. These predictions are compared with the bottom distribution $\xi b(\xi, Q^2 + m_t^2)$ in the VFNS where $\xi = x(1 + m_t^2/Q^2)$.

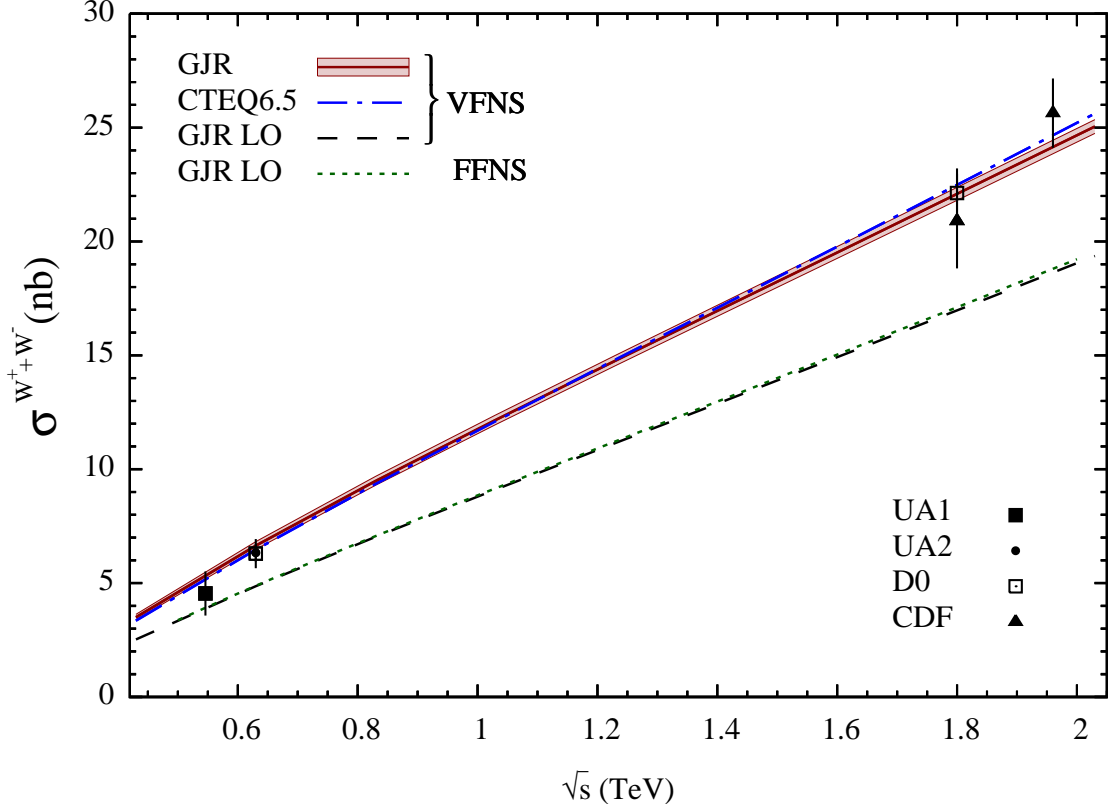


Figure 4: Predictions for the total $W^+ + W^-$ production rates at $p\bar{p}$ colliders with the data taken from [10, 11, 12, 13, 14]. The LO and NLO GJR parton distributions in the VFNS have been generated from the FFNS ones [1] as described in the text. The NLO–VFNS CTEQ6.5 distributions are taken from [15]. The adopted momentum scale is $\mu_R = \mu_F \equiv \mu = M_W$. The scale uncertainty of our NLO GJR predictions, due to varying μ according to $\frac{1}{2}M_W \leq \mu \leq 2M_W$, amounts to less than 2% at $\sqrt{s} = 1.96$ TeV, for example. The shaded region around our central GJR predictions is due to the $\pm 1\sigma$ uncertainty implied by our dynamical NLO parton distributions [1].

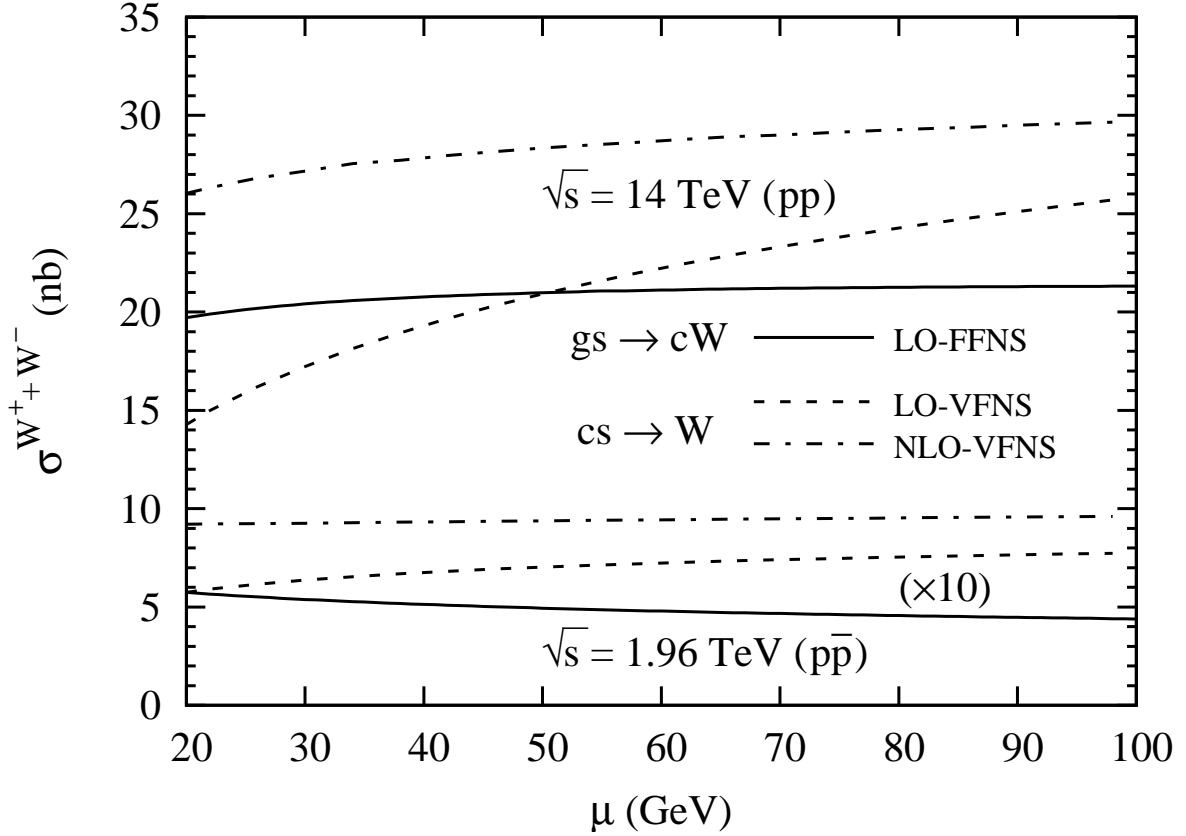


Figure 5: The scale dependence ($\mu_R = \mu_F \equiv \mu$) of the LO-FFNS contribution to the total $W^+ + W^-$ production rate due to the subprocess $gs \rightarrow cW$ compared to the LO and NLO ones in the VFNS due to $cs \rightarrow W$ fusion. The results refer to the pp -LHC ($\sqrt{s} = 14$ TeV) and to the $p\bar{p}$ -Tevatron ($\sqrt{s} = 1.96$ TeV) with the latter ones being multiplied by a factor of 10 as indicated.

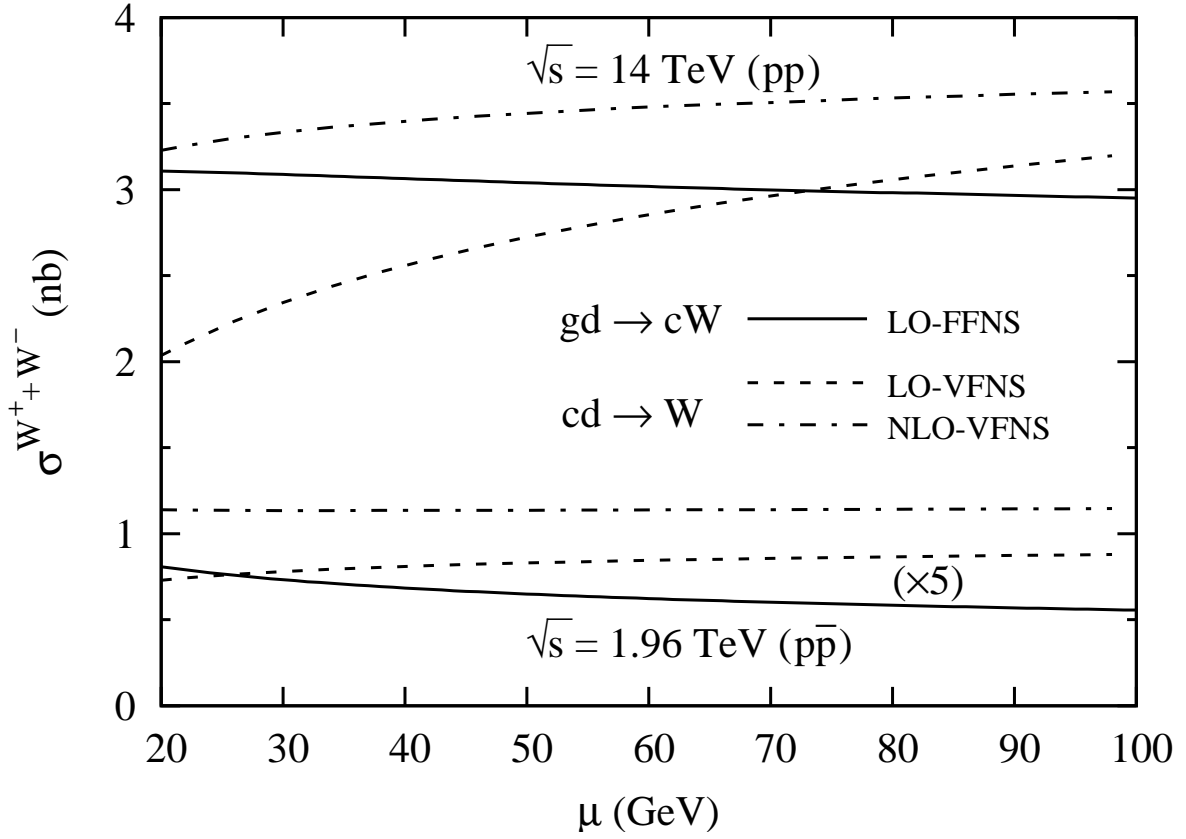


Figure 6: As in Fig. 5 but for the FFNS subprocess $gd \rightarrow cW$ to be compared with $cd \rightarrow W$ in the VFNS. The results for the Tevatron ($\sqrt{s} = 1.96$ TeV) are multiplied by a factor of 5 as indicated.

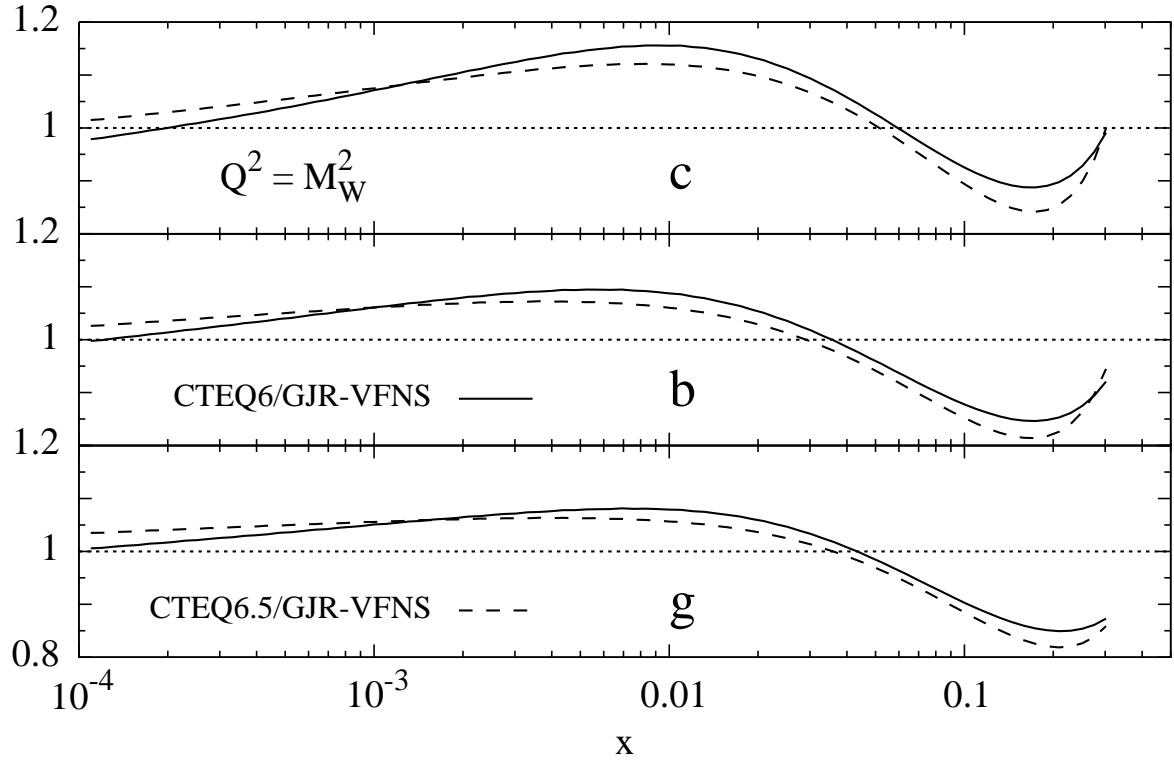


Figure 7: Comparing our present (GJR-VFNS) dynamical parton distributions generated in the VFNS at $NLO(\overline{MS})$ with the ones of CTEQ6 [26] and CTEQ6.5 [15] at $Q^2 = M_W^2$.